Nanoscale

ROYAL SOCIETY OF CHEMISTRY

MINIREVIEW

View Article Online
View Journal | View Issue

Cite this: *Nanoscale*, 2022, **14**, 12560

Recent progress on bioimaging strategies based on Janus nanoparticles

Zheyi Li,[a] Zhiqiang Gao,*[b] Cong Wang,*[a] Danqing Zou,[a] Huan Zhou,[a] Yang Yi,[a] Jun Wang*[c] and Lei Wang *[b]

Received 9th June 2022,
Accepted 10th August 2022

DOI: 10.1039/d2nr03186h

rsc.li/nanoscale

Janus nanoparticles refer to a kind of asymmetric-structured nanoparticles composed of two or more distinct sides with differences in chemical nature and/or polarity on each side and thus can integrate two or more properties in one single particle. Due to their unique structure and surface properties, Janus nanoparticles have shown broad application potentials in optics, nuclear magnetic resonance, multi-mode imaging, and other fields. Unlike traditional contrast agents used in biological imaging, Janus nanoparticles are asymmetrically and directionally oriented to ensure stable partitioning of individual nanoparticles while integrating more functions. Much advancement have been carried out in the past few years, with some studies partially covering bioimaging applications. However, to our best knowledge, there are still no review papers specifically dedicated to the bioimaging applications with Janus nanoparticles. Bearing this in mind and taking the current challenges in this field into consideration, herein, we discuss representative approaches orchestrated for bioimaging applications, with the focus on the improvement of imaging quality brought by Janus nanoparticles and the development of multifunctional nanoplatforms in biological imaging fields, such as theranostics and therapies. Finally, based on the research experience of our group in this field, prospects for future research trends are put forward to provide new ideas for designing new Janus nanoparticles for clinical bioimaging.

[a]*School of Electronic and Information Engineering, School of Chemistry and Chemical Engineering, Harbin Institute of Technology, Harbin 150001, China. E-mail: kevinwang@hit.edu.cn, leiwang_chem@hit.edu.cn*
[b]*School of Aeronautics, Harbin Institute of Technology, Harbin 150001, China. E-mail: gao_zhiqiang@hit.edu.cn*
[c]*School of Instrumentation Science and Engineering, Harbin Institute of Technology, Harbin 150001, China. E-mail: wang_jun@hit.edu.cn*

Introduction

In recent years, with the aggravation of environmental pollution and the change in lifestyle, human beings are faced with more and more diseases. Moreover, the prevalence of

Zheyi Li

Zheyi Li received the B.S. degree in Electronic and Communication Engineering from Harbin Institute of Technology (HIT), Harbin, China, in 2021. She is currently pursuing the M.S. degree in Electronic and Communication Engineering at Harbin Institute of Technology, Harbin, China, under the co-supervision of Prof. Cong Wang and Prof. Lei Wang. Her research interests include the study of microwave biosensors and microwave gas sensors.

Cong Wang

Cong Wang was born in Qingdao, Shandong, China, in 1982. He received the B.S. degree in Automation Engineering from Qingdao Technological University, China, in 2005, and the M.S. and Ph.D. degrees in Electronic Engineering from Kwangwoon University, South Korea, in 2008 and 2011, respectively. Since 2016, he has been with the Department of Microwave Engineering at HIT, where he is currently a full professor. His interests include nanoparticle design and synthesis, microwave and mm-wave active/passive device design and fabrication, microwave humidity sensors, and biosensors.

cancer, diabetes, coronary heart disease, and other diseases is increasing yearly.[1,2] It has been reported that the curing rate of multiple diseases will be significantly improved with early detection and timely treatment.[3,4] As one of the main methods for early diagnosis of diseases, bioimaging technology plays a significant role in screening high-risk groups, preventing individual disease onset, as well as in the early diagnosis of diseases and monitoring the therapeutic effect. Considering the special medical requirements of different organs, appropriate strategies for clinical and biomedical imaging should be well developed and improved, with enhanced imaging efficiency and accuracy of diagnostic results (Fig. 1). Currently, the commonly used contrast agents (Fe_3O_4, Au, *etc.*) are limited by their isotropic properties, resulting in a relatively single imaging mode and limited resolution. Compared with these contrast agents, Janus nanoparticles (JNPs) or patchy nanoparticles exhibit unique properties: (i) compared with single-component nanoparticles, JNPs possess two or more distinct regions with differences in chemical nature and/or polarity in each region, thus offering the possibility for multimodal imaging; (ii) compared with other random hybrid structures or core@shell hybrid nanoparticles, JNPs ensure the stability of the performance of each region to the greatest extent because of the regional isolation brought by the unique structure. Although JNPs combine multiple components together, their optical, magnetic, and other properties related to bioimaging are not lost or interfered; (iii) compared to multifunctional non-Janus NPs, JNPs are prone to asymmetrical modifications to offer easy and selective functionalization, which could facilitate other biomedical functions without sacrificing the original imaging accuracy. Thereby, the unique advantages brought by JNPs would be able to potentially provide revolutionary development in the bioimaging field.

Based on the above merits of JNPs, much effort has been spent in this field in the past decade, which has been partially covered by some review papers.[5–9] However, there is still

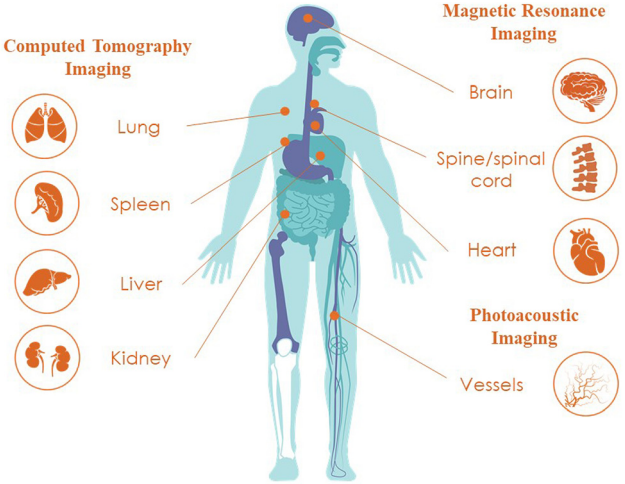

Fig. 1 Human organs and their corresponding preferred bioimaging methods.

no specific review paper that focus on the bioimaging strategies based on JNPs. Bearing it in mind and considering the current challenges, this paper focuses on the discussion of JNPs orchestrated in the field of biological imaging. Regarding the preparation methods, several approaches have been developed, such as the Pickering emulsion method,[10] self-assembly method,[11] seed polymerization,[12] nucleation growth methods,[13] microfluidics method,[14,15] phase separation method,[16] *etc.*, which could be referred to some excellent review articles for details;[17–19] thus, the fabrication techniques are out of the focus of this review paper. Notably, this work also analyses the advantages of JNPs with special optical, electrical, and magnetic properties employed as biological imaging contrast agents for the improvement of imaging quality, resolution, or additional analytical or therapeutic functions. Finally, based on the research experience and problems

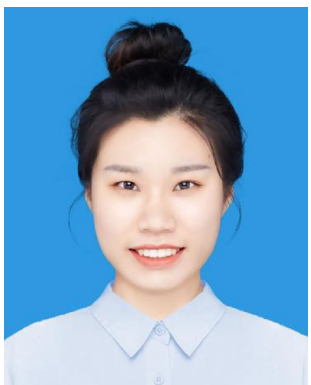

Danqing Zou

Danqing Zou was born in Shen Yang, Liao Ning Province, China in 1998. She received the B.S. degree in Electronic and Communication Engineering from HIT, Harbin, China, in 2020. She is currently pursuing the M.S. degree in Electronic and Communication Engineering at HIT. Her research interests include the study of integrated passive device design and fabrication and microwave humidity sensors.

Lei Wang

Lei Wang received his Ph.D degree from HIT in 2015, with studies at University of Maryland (College Park, USA) under the supervision of Prof. Zhihong Nie, and University of Leeds (UK) under the supervision of Prof. Stephen Evans, respectively. After working as Marie Curie Fellow in Prof. Samuel Sanchez's group at IBEC, Spain (2017–2019), he was appointed as Associate Professor at HIT. Currently, his research interest includes the application of biomaterial self-assembly based on various nanoparticles in the fields of micro/nanomotors, biosensors and biomimetics.

faced by our group, we summarize the current research challenges and propose an outlook on this field, hoping to provide fundamental guidelines for future developments.

Optical imaging

Biological optical imaging refers to a method of imaging cells, tissues, or organisms for optical detection to obtain biological information, which is real-time, non-invasive, and intuitive. According to the imaging mechanisms, biological optical imaging can be classified into fluorescence imaging (FLI), photoacoustic (PA) imaging, optical tomography, *etc*. Therefore, we are going to discuss the application of JNPs orchestrated in the bioimaging field in the following sections.

Fluorescence imaging

Fluorescence imaging has attracted extensive attention in the field of biological imaging because of its high sensitivity and non-invasive properties. The fluorescence signals for bioimaging are derived from the interaction between photons and biological tissues, such as reflection, absorbance, and scattering. Thus, the imaging quality and resolution of fluorescence imaging are largely restricted by the tissue penetration depth of light, especially for *in vivo* imaging, which could not fulfil the practical requirement in the early disease diagnosis. To address this issue, JNPs combined with noble metals such as Au and Ag could be good candidates due to their tunable surface plasmon resonance in the visible to NIR spectral region. Thereby, Ag was employed for two-photon fluorescence imaging previously.[20] In this case, Fe_3O_4–Ag JNPs were designed and prepared, and after the nanoparticles were ingested by macrophages, strong two-photon fluorescence was observed under the excitation of femtosecond infrared laser (900 nm), thus realizing the cell selection and separation. However, the cytotoxic effect of Ag ions released by the nanoparticles limited the *in vivo* imaging applications. To further improve the agents' biocompatibility, Au–MnO@SiO_2 JNPs were designed (Fig. 2(A)), in which the toxicity was significantly reduced by silica coating.[21] As shown in Fig. 2(B), Au–MnO@SiO_2 JNPs were fabricated by the reverse microemulsion technique, and strong two-photon activity was observed at 970 nm excitation wavelength in kidney cancer cells and HeLa cells (Fig. 2(C)). The cell viability assay (for 24 h, 37 °C) revealed that the Au–MnO@SiO_2 JNPs at a concentration of 100 μg mL^{-1} were non-cytotoxic with a cell survival percentage of 94.4 ± 4.7%. With a similar concept, Susewind *et al.*[22] coated ZnO with SiO_2 to protect its stability in the biological environment and improve its biocompatibility. Their study focused on nanorod-like Au–ZnO@SiO_2 JNPs, of which the Au part was used for dark field scattering imaging, and the ZnO part was used to enhance two-photon imaging performance. Au–ZnO@SiO_2 JNPs exhibited good biocompatibility with the silica coating (cell viability over 90%), compared with pure ZnO nanoparticles (cell viability of 20%), thus providing great potential for *in vivo* applications.

The development of modern medical fluorescence imaging has put forward higher requirements for achieving higher resolution and the function of auxiliary diagnosis and treatment at the same time, which could be addressed through the design of the Janus structure. JNPs loaded with UCNPs multiphoton probes realized high-precision imaging of macromolecular vascular scan in the mouse brain after processing with the Richardson–Lucy algorithm.[23] In addition, JNPs can combine fluorescent materials and photothermal therapy by asymmetric structure. For example, Rhodamine B (RhB) was introduced to gold nanorod–mesoporous silica JNPs[24] (Fig. 3 (A) and (B)) and offered a significant photothermal effect (Fig. 3(C)). After injected into the liver, spleen, heart, lung, kidney, and tumour tissue, the nanoparticles could accumulate in the cells of tumour tissue. Most cells died after laser irradiation, while in the control group without NIR laser, only a few cells turned blue by treatment with 0.4% trypan blue for 10 min. It can be seen that the absorption rate of particles has a significant impact on fluorescence imaging and the photothermal treatment effect. To further improve the therapeutic effect, bionics was applied to study the influence of particle shape on absorption rate.[25] A "tadpole-like" JNP was prepared, which could adjust the particle absorption rate of cells by changing the tail length. Both the head and tail of the particle could be modified with fluorescent materials. In addition, the gold coating on the particle's head allows it to effectively kill cancer

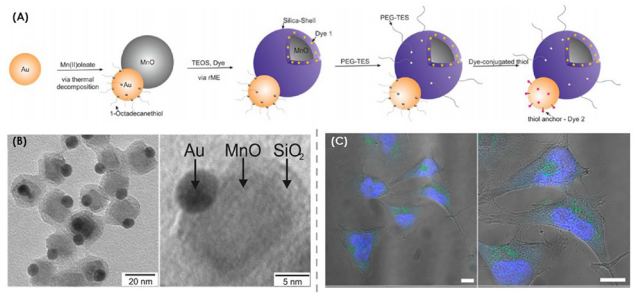

Fig. 2 (A) Scheme showing the synthesis of Au@MnO heterodimer and silica encapsulation; (B) TEM image of Au–MnO@SiO_2 nanoparticles; (C) confocal laser scanning microscopy image of HeLa cells incubated with Au–MnO@SiO_2 for 24 h at 37 °C. Adapted from ref. 21 with permission. Copyright © 2014, American Chemical Society.

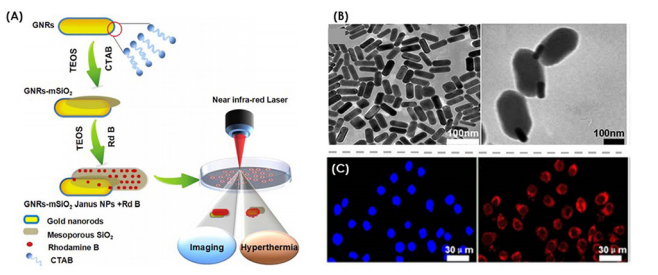

Fig. 3 (A) Schematic diagram of synthesis and application of Janus NPs, (B) TEM image of GNRs-mSiO_2 Janus NPs, (C) confocal laser scanning microscope image of HepG2 cells ingesting JNPs. Adapted from ref. 24 with permission. Copyright © 2015, AIP Publishing.

cells by NIR photothermal properties, thus providing a good example for endowing multiple functions to a single particle.

Photoacoustic imaging

Photoacoustic (PA) imaging, also called optoacoustic or thermoacoustic imaging, has emerged as a promising non-invasive imaging modality, combining the spectral selectivity of molecular excitation by laser light and the high resolution of ultrasound imaging.[26–28] As a new diagnostic imaging method, PA imaging requires contrast agents with strong NIR absorbances to further improve their imaging performance. Compared to other PA imaging contrast nanoprobes, JNPs could offer orthogonal modifications to improve PA conversion efficiency and the depth of penetration to acquire more information about the biosystem. Moreover, the introduction of JNPs into photoacoustic imaging enables the development of a multifunctional nanoparticle platform with therapeutic functions while enhancing high imaging resolution. As is known to all, silver sulfide has been particularly attractive due to its high fluorescence quantum yield and low toxicity in the NIR-II window. However, its lack of disease-specific activation properties limited its application in disease diagnosis. Therefore, Ag/Ag_2S JNP was produced by a one-step synthesis that responds to H_2O_2,[29] shown in Fig. 4(A). The nanoparticles had the advantages of excellent fluorescence properties and showed an activated photoacoustic imaging mechanism (Fig. 4 (B)) and the potential for non-invasive localization and diagnosis of diseases *in vivo*, such as liver injury and cancer. In addition to silver sulfide, gold nanoparticles could efficiently convert light energy into heat, providing high contrast in PA imaging. To utilize its local surface plasmon resonance effect for high-quality imaging, GNPs coated with anisotropic silica nano-shells were synthesized[30] with good PA imaging ability demonstrated by experiments in mice. The aggregation of JNPs could be controlled to amplify photoacoustic signals in the near-infrared region. The ability to modulate JNP aggregation makes a significant contribution to higher resolution and deeper penetration of photoacoustic imaging, which is attractive for diagnostic imaging.

To further explore the potential of gold nanoparticles in gene therapy, a Janus-structured chitosan/gold nanohybrid (J-ACP) was reported to show great photothermal effect in culture medium with incubated cells,[31] which had great potential in realizing complementary photothermal therapy (PTT)/gene therapy guided by photoacoustic (PA) imaging. Furthermore, a unique dopamine-mesoporous calcium phosphate (PDA-mCaP) JNP realized the function of drug delivery on account of hollow cavities (Fig. 5(A)).[32] The PDA side was modified with indocyanine green and polyethylene glycol mercaptan, and the unique hollow structure of the particle (Fig. 5(B)) makes it capable of drug loading. The particle had good photothermal treatment ability, near-infrared and pH dual-controlled drug release ability, and PA imaging ability (Fig. 5(C)). This provides a feasible way for the development of multifunctional nanoplatforms and the research for new generation cancer drugs.

Magnetic resonance imaging

Magnetic resonance imaging (MRI) is one of the main imaging techniques used in clinical medicine. It has been widely used in the diagnosis of liver, lung, breast, and other viscera tumours because of its high contrast, high spatial resolution, and many other advantages.

MRI imaging quality plays an important role in the early diagnosis of cancer. In order to improve the resolution, contrast agents could be employed during MRI scanning. However, *T*1 contrast agents have poor sensitivity for molecular imaging, and *T*2 or *T*2* contrast agents have difficulty in distinguishing from naturally low MRI signal tissues (*e.g.*,

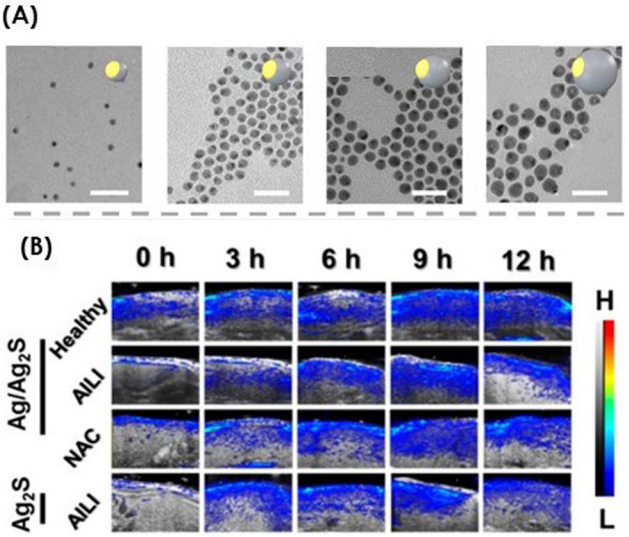

Fig. 4 (A) TEM images of Ag/Ag_2S JNPs with different sizes; (B) corresponding PA imaging of different experimental groups (excitation at 808 nm). Adapted from ref. 29 with permission. Copyright © 2021, American Chemical Society.

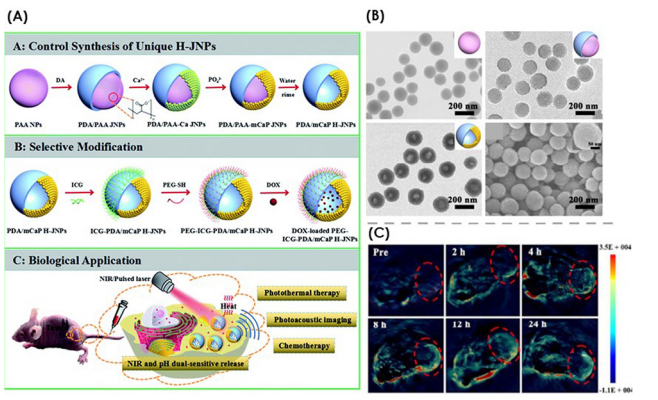

Fig. 5 (A) PA imaging guided chemo-photothermal synergistic cancer therapy, (B) TEM images of PAA NPs, PDA/PAA JNPs, and magnified SEM images of PDA/mCaP H-JNPs, (C) PA images of nude mice at various time points before and after intravenous injection of H-JNPs. Adapted from ref. 32 with permission.

bone, lung). JNPs are attractive candidates for MRI contrast agents, which could ameliorate these deficiencies by modifying the size and morphology to enhance the contrast between normal and diseased tissues or developing *T*1–*T*2 dual mode contrast agents to acquire complementary imaging information. To this end, Fe_3O_4–Au nanoparticles were designed to provide a higher contrast in *T*2-weighted MRI images,[33] which could be attributed to the high magnetization of Fe_3O_4 crystal and the large magnetic field gradient at the corner and edge of the octahedron (Fig. 6). In order to combine the advantages of *T*1 and *T*2-weighted images, PEG-stabilized $MnFe_2O_4$–MnO nanoparticles based on Janus structure were constructed successfully,[34] which can be used as *T*1 and *T*2 dual-mode magnetic resonance enhanced contrast agent. PEG makes the nanosystem stable in aqueous solutions, which is conducive to its application in the biomedical field. MnO and $MnFe_2O_4$ are used to enhance the contrast of *T*1 and *T*2 weighted MRI images, respectively. In this report, the particle had the ability to achieve dual-mode MRI imaging, which was verified *in vivo* and *in vitro* experiments, therefore providing ideas for the design of new dual-mode MRI contrast agents.

Recently, molecular imaging, diagnostics, and therapy of cancer based on nanomaterials have become a promising field, which requires MRI contrast agents to be multifunctional. Based on this idea, Janus-structured Fe_3O_4–TiO_2 nanoparticles were reported for the first time.[35] Fe_3O_4 and TiO_2 materials were used as MRI contrast agents and inorganic photosensitizers of PDT, respectively. The survival rate of MCF-7 cells after UV light exposure was down to about 85%–39%, compared with the cells without radiation, which proved the potential application of the particle in MRI and PDT combined diagnosis and treatment. Mn_3O_4–TiO_2 nanoparticles with Janus structure were also prepared to inactivate tumour cells under low-intensity UV irradiation (Fig. 7(A)) with excellent properties for PDT.[36] As shown in Fig. 7(B), the nanoparticles showed promising tumour ablation performance in PDT at a low intensity of UV irradiation. In addition to PDT therapy, cancer treatment could be achieved through magnetic hyperthermia. One such work[37] developed Fe–Au nanorod JNPs that could be used for cell targeting, therapy, and bioimaging. The functional material HRG allowed specific recognition of tumour cells, and the magnetic response of iron material could realize not only imaging function, but also magnetic hyperthermia for tumour cells.

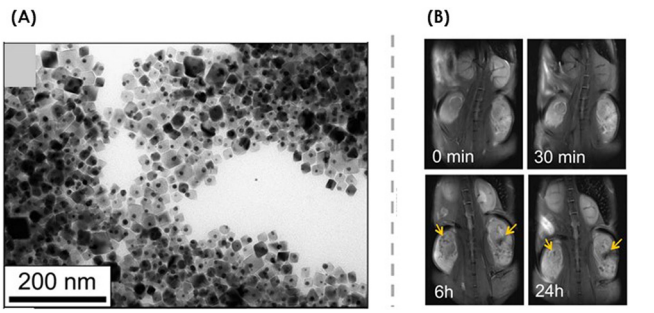

Fig. 6 (A) TEM images of Fe_3O_4–Au hybrid NPs, (B) representative *T*2-weighted images of mice captured before and 24 h after injection of NPs. Adapted from ref. 33 with permission.

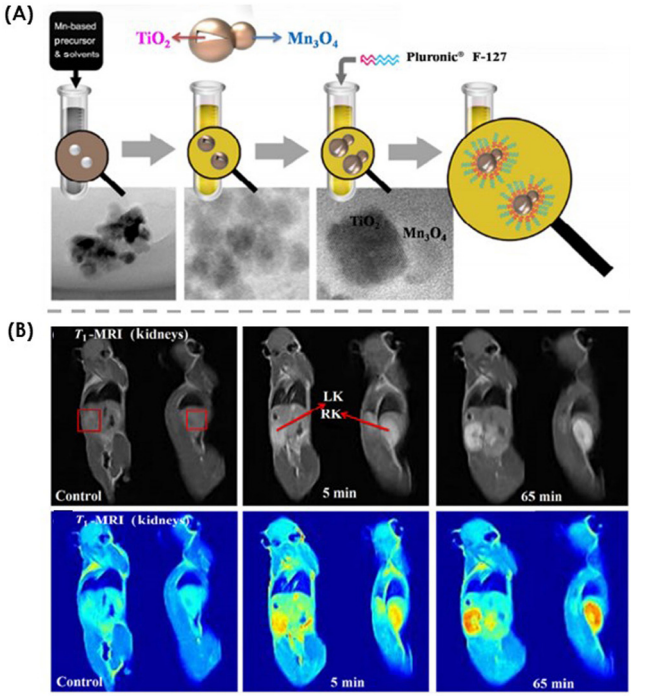

Fig. 7 (A) Mn_3O_4–TiO_2 Janus nanostructure and schematic diagram of MRI and PDT application, (B) *T*1-weighted MRI images of the left and right kidneys of mice before, 5, and 65 min after injection. Adapted from ref. 36 with permission. Copyright © 2018, Tsinghua University Press and Springer-Verlag GmbH Germany, part of Springer Nature.

Computed tomography imaging

Computed tomography (CT) imaging has been widely used in the field of disease diagnosis due to its advantages of fast scanning time and clear images. Gold nanoparticles have been commonly used as contrast agents for CT imaging because of their high absorption coefficient of X-rays. JNPs based on gold nanoparticles could further improve the contrast of CT images and improve sensitivity by combining with specific targeting materials. To this end, gold nanoparticles have been applied to synthesize JNPs for CT imaging and have other functions such as tumour cell targeting and controlled drug release.[38] As shown in Fig. 8, one hemisphere of each Janus nanosphere contained gold nanoparticles as an X-ray contrast agent, whereas the other hemisphere was modified with folic acid (FA) and antitumor drugs to complete the targeting and controlled release for liver cancer cells. To further improve stability and biocompatibility, Wang's team[39] used calcium phosphate to develop folic acid–Au@poly(acrylic acid)/mesoporous calcium phosphate JNPs (FA–Au@PAA/mCaP JNPs), which showed a good pH response. The gold side was used for CT imaging and tumour cell targeting, while the mesoporous calcium phosphate side realized pH response and drug deliv-

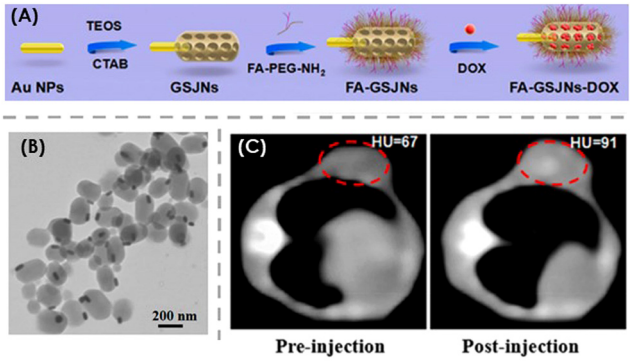

Fig. 8 (A) Synthesis process of DOX loaded mesoporous silicon JNPs, (B) TEM images of FA-GSJNs, (C) *in vivo* CT images of SMMC-7721 tumour-bearing nude mice at 24 h post-injection with GSJNs-DOX. Adapted from ref. 38 with permission. Copyright © 2017, American Chemical Society.

ery. Another non-toxic nanoparticle for diagnostic and therapeutic drugs is Prussian blue nanoparticles (PB NPs). A unique PB@PAA/AU-A JNP[40] was reported, which combined enhanced photothermal therapy, effective chemotherapy, and diagnostic imaging. These nanoparticles maintained the original photothermal properties of PB and Au domains while the heterostructure added the function of drug loading to promote tumour suppression. The above articles realized the multifunctional nanoparticles based on Janus structure, proposing a feasible strategy for the development of multifunctional nanoplatforms for medical diagnosis.

In addition to the above imaging methods, researchers also reported JNPs in magnetic particle imaging,[41] ultrasound imaging,[42,43] positron emission tomography imaging[44] and other fields. In addition, the electroluminescence properties,[45] magnetic-luminescence properties,[46] up-conversion luminescence properties,[23] and SERS properties[47] can also be combined with a biological imaging function, which has certain application potential in biological imaging, targeted drugs, and image-guided therapy.

Multi-mode imaging

The disadvantages of single-mode imaging in sensitivity, resolution, imaging time, and cost limit its further development in the field of biological imaging. In order to overcome the above limitations, it is urgent to develop multi-mode imaging technology with high sensitivity and high resolution, which combines the advantages of various imaging technologies. Due to its special structure, JNPs can be anisotropic in composition, shape, and surface properties. As a result, it could combine the advantages of different imaging methods more conveniently without affecting the original imaging quality, which has more potential to be contrast agents for multi-mode imaging technology compared with other nanoparticles. Take dual-mode imaging as an example, since MRI is one of the most powerful imaging techniques, offering superior contrast compared with CT. While CT instruments are more available, efficient, and less costly than MRI platforms, a dual contrast agent for both MRI and CT could compensate for the limitations of both imaging methods above. In order to verify the idea, polymer-coated Au–Fe_3O_4 dumbbell-shaped JNPs were developed for the first time.[48] The nanoparticles showed high CT attenuation, which could be attributed to the gold layers, and provided a good MRI signal owing to the iron oxide nanoparticle. A further advancement of these JNPs has been the recent improvement of imaging performance by modifying functional materials.[49] Folic acid on the surface of Au–Fe_3O_4@C nanoparticles improved the particle's CT imaging contrast and the ability to target cancer cells. The Fe_3O_4@C side can be used as an MRI contrast agent and drug carrier. In addition, the function of drug loading was added on the basis of multi-mode imaging. These JNPs provided a nanoplatform for dual-modal CT and MR imaging-guided actively targeted chemo-photothermal synergistic cancer therapy. Considering the severe drug resistance of single drugs in treating cancers, the synergistic combination of two therapeutic agents has attracted more attention, especially in an appropriate administrated sequence. Consequently, a unique PCL-AuNC/$Fe(OH)_3$-PAA JNP was designed to simultaneously preserve the hydrophilic and hydrophobic drug for the first time (Fig. 9(A)).[50] Owing to the heterostructure, independent pH, and NIR sensitive properties, the nanoparticles could release the drug in a particular sequence. In addition, cancer therapy could be guided effectively by the excellent CT/MR imaging capabilities from AuNC and $Fe(OH)_3$ (Fig. 9(B)), which showed better tumour inhibition than the solo drug, cocktail, and dual drug treated groups. In addition to dual-mode imaging, the researchers also combined other imaging methods with CT and MRI to achieve three-mode imaging for a faster, more accurate, and safer prognosis. A PEG-Au-Fe_3O_4 JNP[51] showed a significant photothermal effect with a 40% calculated photothermal transduction efficiency with the ability of triple-modal MR imaging/PA imaging/CT *in vitro*, demon-

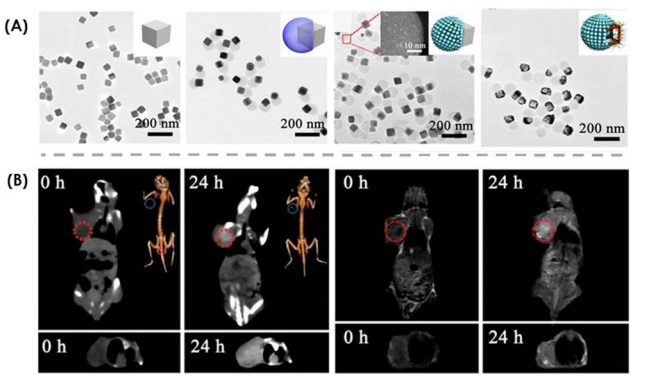

Fig. 9 (A) TEM images of AgNCs, AgNC/PAA JNPs, AgNC/$Fe(OH)_3$-PAA JNPs, and AuNC/$Fe(OH)_3$-PAA JNPs, (B) cross-sectional CT images and *T*1 weighted MR images of mouse collected pre and 24 h post-intravenous injection. Adapted from ref. 50 with permission. © 2018 Elsevier Ltd. All rights reserved.

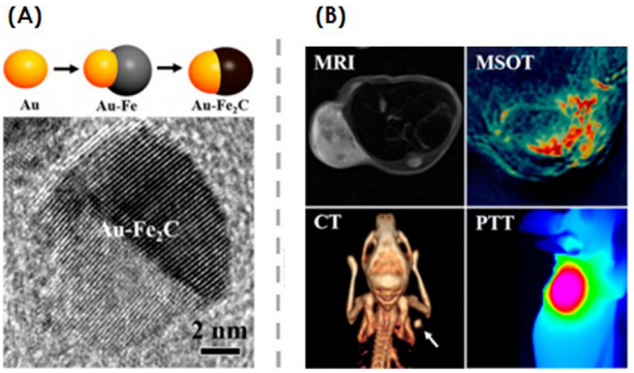

Fig. 10 (A) Schematic diagram of Au–Fe_2C particle preparation. (B) (MSOT)/CT/MRI three-mode and PTT images. Adapted from ref. 52 with permission. Copyright © 2017, American Chemical Society.

strating the feasibility of JNPs as three-mode imaging contrast agents. In order to improve the ability of nanoparticles to target cancer cells, Au–Fe_2C nanoparticles were modified with affinity protein[52] (Fig. 10(A)), which showed great potential as an effective contrast for (MSOT)/CT/MRI three-mode imaging (Fig. 10(B)). In addition to three-mode imaging functions, the nanoparticles further incorporated tumour cell targeting and photothermal therapy. The results showed that the JNPs could target and kill tumour cells through laser radiation in the therapeutic period. It is notable that an Au–Fe_3O_4 JNP was developed as a contrast agent for multi-mode imaging,[53] which demonstrated the imaging properties of MRI, CT, PA, optical microscope under dark and bright field, transmission electron microscope, and SERS. It further indicated that JNPs had unique advantages in the field of multi-mode imaging.

In addition to the above multi-mode imaging methods, JNPs can also be used as contrast agents for multi-mode imaging technologies such as MRI combined with optical imaging,[54–58] CT imaging combined with optical imaging,[59] and PA combined with ultrasonic imaging,[60] which has great application potential in the field of biological imaging.

In the field of biological imaging, JNPs have been widely used as contrast agents in multiple imaging methods. Table 1 summarizes the representative applications of JNPs in biological imaging in recent years. JNP has unique advantages in the field of multimodal imaging due to its special structure, but the multimodal imaging potential of the particle has not been fully utilized. In the future, we can combine JNPs and multi-mode imaging by optimizing the preparation method or proposing new ideas to improve the imaging performance.

Table 1 Representative applications of Janus nanoparticles in bioimaging

Entry	Composition	Morphology	Imaging approach	Ref.
1	Au–ZnO@SiO_2	Rod	FLI	19
2	GNRs–mSiO_2	Rod	FLI	20
3	Polymer–SiO_2@Au	Tadpole	FLI	21
4	Au–SiO_2	Hybrid	FLI	24
5	Mn_3O_4–TiO_2	Dumbbell	MRI	35
6	FA–Au–mSiO_2–DOX	Spindle	CT	37
7	FA–Au@PAA/mCaP	Dumbbell	CT	38
8	FA–Au/Fe_3O_4@C	Dumbbell	CT/MRI	49
9	PCL-AuNC/$Fe(OH)_3$-PAA	Dumbbell	CT/MRI	50
10	PEG-Au–Fe_3O_4	Dumbbell	CT/MRI/PA	51
11	Fe_3O_4–Au	Star	CT/MRI/PA/SERS	53

Conclusions

In this paper, we discussed the unique properties of JNPs and their advantages and representative applications in the field of bioimaging in order to provide guidelines for the design and utilization of bioimaging nanoparticles in the future. JNPs consist of asymmetric structures and compositions with multiple properties, such as two or more different optical, magnetic, or electrical properties together, therefore realizing the enhancement of imaging resolution, developing multifunctional theranostic nanoplatforms (like a single system with biological imaging, drug delivery, and photothermal therapy together), and fabricating multi-mode imaging contrast agents. In addition, JNPs greatly improve the biocompatibility of contrast agents and reduce the damage during *in vivo* imaging by combining materials with low biotoxicity.

However, the research and development of biological imaging using Janus nanomaterials is still in the infancy stage. Despite the common challenges to efficiently and massively prepare Janus materials with stable structure and properties, there are still several challenges in the bioimaging field, such as but not limited to: firstly, the biocompatibility of contrast nanoparticles is crucial in the field of bioimaging. Taking fluorescence imaging as an example, some biotoxic fluorescent dyes could be wrapped in JNPs to reduce its damage, which could not be used in living organisms previously. Thereby, the biocompatibility of materials, the distribution after injecting JNPs into tissue or body, and the safety of degradation will also be the focus of future work. Secondly, the resolution is another focus of bioimaging. In addition to the convenience of modifying various functional groups to increase the resolution limit of single-mode bioimaging technology, JNPs provide a convenient way to achieve dual-mode or even multi-mode imaging. The benefit of JNPs in combining specific advantages of different imaging techniques in spatial resolution, penetration depth, imaging time, *etc.*, has not been fully used for the improvement of comprehensive imaging quality. Thirdly, owing to the easy and selective functionalization, JNPs could be designed to respond to different environments and aggregate in specific tissues or organs, which could be used in local imaging or real-time tracking imaging of different organs in biosystems. However, designing JNPs with the ability of targeted recognition and tunable aggregation in specific biological tissues is still challenging. Fourthly, the construction of multifunctional JNPs platform based on bioimaging function has become the mainstream due to the requirement for early diagnosis of diseases.

It also attracted people's interest in how to balance the role of JNPs in imaging and other functions; thus, it could pursue more sophisticated functions for auxiliary disease diagnosis and treatment while serving as high-performance imaging contrast agents. In addition, Janus micro/nanomotors, with enhanced targeting and collective behavior, could provide new approaches to improve the bioimaging effect and control the distribution of JNPs.

Author contributions

Z. Li, investigation, writing – original draft. Z. Gao, investigation. C. Wang, investigation, writing – review & editing, supervision, funding acquisition. D. Zou, investigation. H. Zhou, investigation. Y. Yi, investigation. J. Wang, investigation, writing – review & editing. L. Wang, investigation, conceptualization, writing – review & editing, supervision, funding acquisition.

Conflicts of interest

There are no conflicts to declare.

Acknowledgements

The authors appreciate the financial support from the National Key Research and Development Program of China (No. 2019YFE0121800, 2021YFF0603500), NSFC (No. 52073071, 51703043), and general and special funding from the Postdoctoral Science Foundation of China (2017M611367 and 2020T130144).

References

1 A. Collier, C. Meney, M. Hair, L. Cameron and J. G. Boyle, *J. Diabetes Invest.*, 2020, **11**, 55–61.
2 P. Saeedi, I. Petersohn, P. Salpea, B. Malanda, S. Karuranga, N. Unwin, S. Colagiuri, L. Guariguata, A. A. Motala, K. Ogurtsova, J. E. Shaw, D. Bright and R. Williams, *Diabetes Res. Clin. Pract.*, 2019, **157**, 107843.
3 N. Hawkes, *Br. Med. J.*, 2019, **364**, l860.
4 P. Karimi, F. Islami, S. Anandasabapathy, N. D. Freedman and F. Kamangar, *Cancer Epidemiol. Biomarkers Prev.*, 2014, **23**, 700–713.
5 X. Zhang, Q. Fu, H. Duan, J. Song and H. Yang, *ACS Nano*, 2021, **15**, 6147–6191.
6 X. Li, L. Chen, D. Cui, W. Jiang, L. Han and N. Niu, *Coord. Chem. Rev.*, 2022, **454**, 214318.
7 Y. Yi, L. Sanchez, Y. Gao and Y. Yu, *Analyst*, 2016, **141**, 3526–3539.
8 Z. Rahiminezhad, A. M. Tamaddon, S. Borandeh and S. S. Abolmaali, *Appl. Mater. Today*, 2020, **18**, 100513.
9 H. Su, C. A. H. Price, L. Jing, Q. Tian, J. Liu and K. Qian, *Mater. Today Bio*, 2019, **4**, 100033.
10 Ł. Baran, M. Borówko and W. Rżysko, *J. Phys. Chem. C*, 2020, **124**, 17556–17565.
11 R. Deng, H. Li, J. Zhu, B. Li, F. Liang, F. Jia, X. Qu and Z. Yang, *Macromolecules*, 2016, **49**, 1362–1368.
12 Y. Li, S. Chen, S. Demirci, S. Qin, Z. Xu, E. Olson, F. Liu, D. Palm, X. Yong and S. Jiang, *J. Colloid Interface Sci.*, 2019, **543**, 34–42.
13 B. Shan, Y. Zhao, Y. Li, H. Wang, R. Chen and M. Li, *Chem. Mater.*, 2019, **31**, 9875–9886.
14 Z. Yu, C.-F. Wang, L. Ling, L. Chen and S. Chen, *Angew. Chemie*, 2012, **124**, 2425–2428.
15 L. Wang, Y. Liu, J. He, M. J. Hourwitz, Y. Yang, J. T. Fourkas, X. Han and Z. Nie, *Small*, 2015, **11**, 3762–3767.
16 Y. Zhang, L. Kang, H. Huang and J. Deng, *ACS Appl. Mater. Interfaces*, 2020, **12**, 6319–6327.
17 C. Marschelke, A. Fery and A. Synytska, *Colloid Polym. Sci.*, 2020, **298**, 841–865.
18 A. Walther and A. H. E. Müller, *Chem. Rev.*, 2013, **113**, 5194–5261.
19 J. Hu, S. Zhou, Y. Sun, X. Fang and L. Wu, *Chem. Soc. Rev.*, 2012, **41**, 4356–4378.
20 J. Jiang, H. Gu, H. Shao, E. Devlin, G. C. Papaefthymiou and J. Y. Ying, *Adv. Mater.*, 2008, **20**, 4403–4407.
21 I. Schick, S. Lorenz, D. Gehrig, A.-M. Schilmann, H. Bauer, M. Panthöfer, K. Fischer, D. Strand, F. Laquai and W. Tremel, *J. Am. Chem. Soc.*, 2014, **136**, 2473–2483.
22 M. Susewind, A. M. Schilmann, J. Heim, A. Henkel, T. Link, K. Fischer, D. Strand, U. Kolb, M. N. Tahir, J. Brieger and W. Tremel, *J. Mater. Chem. B*, 2015, **3**, 1813–1822.
23 S. Plunkett, M. El Khatib, İ. Şencan, J. E. Porter, A. T. N. Kumar, J. E. Collins, S. Sakadžić and S. A. Vinogradov, *Nanoscale*, 2020, **12**, 2657–2672.
24 Y. S. Wang, D. Shao, L. Zhang, X. L. Zhang, J. Li, J. Feng, H. Xia, Q. S. Huo, W. F. Dong and H. B. Sun, *Appl. Phys. Lett.*, 2015, **106**, 1–5.
25 H. Kang, S. H. Kim, S. M. Yang and J. H. Park, *J. Mater. Chem. B*, 2014, **20**, 6462–6466.
26 A. B. E. Attia, G. Balasundaram, M. Moothanchery, U. S. Dinish, R. Bi, V. Ntziachristos and M. Olivo, *Photoacoustics*, 2019, **16**, 100144.
27 D. Das, A. Sharma, P. Rajendran and M. Pramanik, *Phys. Med. Biol.*, 2021, **66**, 05TR01.
28 Q. Fu, R. Zhu, J. Song, H. Yang and X. Chen, *Adv. Mater.*, 2019, **31**, 1–31.
29 X. Zhang, W. Wang, L. Su, X. Ge, J. Ye, C. Zhao, Y. He, H. Yang, J. Song and H. Duan, *Nano Lett.*, 2021, **21**, 2625–2633.
30 J. H. Park, D. S. Dumani, A. Arsiwala, S. Emelianov and R. S. Kane, *Nanoscale*, 2018, **10**, 15365–15370.
31 X. Dai, X. Zhao, Y. Liu, B. Chen, X. Ding, N. Zhao and F. J. Xu, *Small*, 2021, **17**, 1–14.
32 M. Zhang, L. Zhang, Y. Chen, L. Li, Z. Su and C. Wang, *Chem. Sci.*, 2017, **8**, 8067–8077.

33 M. V. Efremova, V. A. Naumenko, M. Spasova, A. S. Garanina, M. A. Abakumov, A. D. Blokhina, P. A. Melnikov, A. O. Prelovskaya, M. Heidelmann, Z. A. Li, Z. Ma, I. V. Shchetinin, Y. I. Golovin, I. I. Kireev, A. G. Savchenko, V. P. Chekhonin, N. L. Klyachko, M. Farle, A. G. Majouga and U. Wiedwald, *Sci. Rep.*, 2018, **8**, 1–19.
34 K. Deka, A. Guleria, D. Kumar, J. Biswas, S. Lodha, S. D. Kaushik, S. A. Choudhary, S. Dasgupta and P. Deb, *Dalton Trans.*, 2019, **48**, 1075–1083.
35 L. Zeng, W. Ren, L. Xiang, J. Zheng, B. Chen and A. Wu, *Nanoscale*, 2013, **5**, 2107–2113.
36 M. Z. Iqbal, W. Ren, M. Saeed, T. Chen, X. Ma, X. Yu, J. Zhang, L. Zhang, A. Li and A. Wu, *Nano Res.*, 2018, **11**, 5735–5750.
37 D. Kilinc, A. Lesniak, S. A. Rashdan, D. Gandhi, A. Blasiak, P. C. Fannin, A. von Kriegsheim, W. Kolch and G. U. Lee, *Adv. Healthcare Mater.*, 2015, **4**, 395–404.
38 Z. Wang, D. Shao, Z. Chang, M. Lu, Y. Wang, J. Yue, D. Yang, M. Li, Q. Xu and W. F. Dong, *ACS Nano*, 2017, **11**, 12732–12741.
39 H. Wang, S. Li, L. Zhang, X. Chen, T. Wang, M. Zhang, L. Li and C. Wang, *Nanoscale*, 2017, **9**, 14322–14326.
40 D. Li, A. Bao, X. Chen, S. Li, T. Wang, L. Zhang, J. Ji, Q. Li, C. Wang, Y. Gao, Y. Yang and X. Dong, *Adv. Ther.*, 2020, **3**, 1–10.
41 G. Song, M. Chen, Y. Zhang, L. Cui, H. Qu, X. Zheng, M. Wintermark, Z. Liu and J. Rao, *Nano Lett.*, 2018, **18**, 182–189.
42 K. Tamarov, A. Sviridov, W. Xu, M. Malo, V. Andreev, V. Timoshenko and V. P. Lehto, *ACS Appl. Mater. Interfaces*, 2017, **9**, 35234–35243.
43 Y. Feng, X. Chang, H. Liu, Y. Hu, T. Li and L. Li, *Appl. Mater. Today*, 2021, **23**, 101026.
44 J. Song, L. Lin, Z. Yang, R. Zhu, Z. Zhou, Z. W. Li, F. Wang, J. Chen, H. Yang and X. Chen, *J. Am. Chem. Soc.*, 2020, **141**, 8158–8170.
45 M.-J. Zhu, J.-B. Pan, Z.-Q. Wu, X.-Y. Gao, W. Zhao, X.-H. Xia, J.-J. Xu and H.-Y. Chen, *Angew. Chemie*, 2018, **130**, 4074–4078.
46 Q. Wu, Y. Lin, F. Wo, Y. Yuan, Q. Ouyang, J. Song, J. Qu and K. T. Yong, *Small*, 2017, **13**, 1–13.
47 D. Shao, X. Zhang, W. Liu, F. Zhang, X. Zheng, P. Qiao, J. Li, W. F. Dong and L. Chen, *ACS Appl. Mater. Interfaces*, 2016, **8**, 4303–4308.
48 D. Kim, M. K. Yu, T. S. Lee, J. J. Park, Y. Y. Jeong and S. Jon, *Nanotechnology*, 2011, **22**, 155101.
49 Q. Zhang, L. Zhang, S. Li, X. Chen, M. Zhang, T. Wang, L. Li and C. Wang, *Chem. – Eur. J.*, 2017, **23**, 17242–17248.
50 L. Zhang, M. Zhang, L. Zhou, Q. Han, X. Chen, S. Li, L. Li, Z. Su and C. Wang, *Biomaterials*, 2018, **181**, 113–125.
51 X. Chen, G. Li, Q. Han, X. Li, L. Li, T. Wang and C. Wang, *Chem. – Eur. J.*, 2017, **23**, 17204–17208.
52 Y. Ju, H. Zhang, J. Yu, S. Tong, N. Tian, Z. Wang, X. Wang, X. Su, X. Chu, J. Lin, Y. Ding, G. Li, F. Sheng and Y. Hou, *ACS Nano*, 2017, **11**, 9239–9248.
53 J. Reguera, D. Jiménez De Aberasturi, M. Henriksen-Lacey, J. Langer, A. Espinosa, B. Szczupak, C. Wilhelm and L. M. Liz-Marzán, *Nanoscale*, 2017, **9**, 9467–9480.
54 Y. Liu, X. Yang, Z. Huang, P. Huang, Y. Zhang, L. Deng, Z. Wang, Z. Zhou, Y. Liu, H. Kalish, N. M. Khachab, X. Chen and Z. Nie, *Angew. Chem., Int. Ed.*, 2016, **55**, 15297–15300.
55 S. T. Selvan, P. K. Patra, C. Y. Ang and J. Y. Ying, *Angew. Chemie*, 2007, **119**, 2500–2504.
56 J. Lee, G. Hwang, Y. S. Hong and T. Sim, *Analyst*, 2015, **140**, 2864–2868.
57 C. Xu, J. Xie, D. Ho, C. Wang, N. Kohler, E. G. Walsh, J. R. Morgan, Y. E. Chin and S. Sun, *Angew. Chem., Int. Ed.*, 2008, **47**, 173–176.
58 Y. Zhang, Y. Wan, Y. Liao, Y. Hu, T. Jiang, T. He, W. Bi, J. Lin, P. Gong, L. Tang and P. Huang, *Sci. Bull.*, 2020, **65**, 564–572.
59 A. Sánchez, K. O. Paredes, J. Ruiz-Cabello, P. Martínez-Ruíz, J. M. Pingarrón, R. Villalonga and M. Filice, *ACS Appl. Mater. Interfaces*, 2018, **10**, 31032–31043.
60 J. Ye, Q. Fu, L. Liu, L. Chen, X. Zhang, Q. Li, Z. Li, L. Su, R. Zhu, J. Song and H. Yang, *Sci. China: Chem.*, 2021, **64**, 2218–2229.